THE JOURNAL OF BIOLOGICAL CHEMISTRY VOL. 281, NO. 50, pp. 38244–38256, December 15, 2006

Translesion Synthesis across O^6-Alkylguanine DNA Adducts by Recombinant Human DNA Polymerases*[S]

Received for publication, August 31, 2006, and in revised form, October 10, 2006 Published, JBC Papers in Press, October 18, 2006, DOI 10.1074/jbc.M608369200

Jeong-Yun Choi[‡§1], Goutam Chowdhury[‡1,2], Hong Zang[‡2], Karen C. Angel[‡], Choua C. Vu[¶], Lisa A. Peterson[¶], and F. Peter Guengerich[‡3]

From the [‡]Department of Biochemistry and Center in Molecular Toxicology, Vanderbilt University School of Medicine, Nashville, Tennessee 37232-0146, the [§]Department of Pharmacology, College of Medicine, Ewha Womans University, Seoul 158-710, Republic of Korea, and [¶]Division of Environmental Health Sciences and the Cancer Center, University of Minnesota, Minneapolis, Minnesota 55455

Previous studies have shown that replicative bacterial and viral DNA polymerases are able to bypass the mutagenic lesions O^6-methyl and -benzyl (Bz) G. Recombinant human polymerase (pol) δ also copied past these two lesions but was totally blocked by O^6-[4-oxo-4-(3-pyridyl)butyl] (Pob)G, an important mutagenic lesion formed following metabolic activation of the tobacco-specific carcinogen 4-(methylnitrosamino)-1-(3-pyridyl)-1-butanone. The human translesion pols ι and κ produced mainly only 1-base incorporation opposite O^6-MeG and O^6-BzG and had very low activity in copying O^6-PobG. Human pol η copied past all three adducts. Steady-state kinetic analysis showed similar efficiencies of insertion opposite the O^6-alkylG adducts for dCTP and dTTP with pol η and κ; pol ι showed a strong preference for dTTP. pol η, ι, and κ showed pre-steady-state kinetic bursts for dCTP incorporation opposite G and O^6-MeG but little, if any, for O^6-BzG or O^6-PobG. Analysis of the pol η O^6-PobG products indicated that the insertion of G was opposite the base (C) 5′ of the adduct, but this product was not extended. Mass spectrometry analysis of all of the pol η primer extension products indicated multiple components, mainly with C or T inserted opposite O^6-alkylG but with no deletions in the cases of O^6-MeG and O^6-PobG. With pol η and O^6-BzG, products were also obtained with −1 and −2 deletions and also with A inserted (opposite O^6-BzG). The results with pol η may be relevant to some mutations previously reported with O^6-alkylG adducts in mammalian cells.

Chemical and physical damage to DNA can cause mutations and ultimately cancer, cardiovascular disease, aging, and other diseases (1–4). This damage can result from endogenous agents or exogenous chemicals. Many types of damage are known, and the biological effects can vary considerably. One of the prominent types of damage is alkylation at the O-6 atom of guanine (5, 6). O^6-AlkylG[4] lesions are some of the more mutagenic lesions formed from DNA-alkylating agents (5, 7). The ability of O^6-alkylG adducts to cause mutations has been demonstrated directly in site-specific mutagenesis experiments with defined adducts (8–12). Further support for the view that these are deleterious species derives from the existence of specific DNA repair systems for this type of damage in almost all species, ranging from most bacteria to humans (13, 14).

Different alkylating agents form O^6-alkylG adducts, and structure-activity relationships are important for understanding the basic mechanisms of how DNA polymerases function as well as issues such as carcinogenesis. Studies have been done on the comparative mutagenesis of O^6-MeG, O^6-ethylG, and O^6-BzG[5] lesions in *Escherichia coli* (11), but *in vivo* experiments have caveats about the effects of DNA repair (*e.g.* some O^6-alkylG DNA-alkyltransferases are considerably more proficient with O^6-BzG than O^6-MeG (15)) (Fig. 1). O^6-EthylG and O^6-BzG produce some nontargeted mutations in the H-*ras* gene in Rat4 cells (9). Previous work on blockage and misincorporation opposite O^6-MeG and O^6-BzG has been done in this laboratory with the replicative model polymerases pol T7$^-$ and HIV-1 RT (16) and by others with several DNA polymerases, mostly bacterial (7, 17, 18). Some of the more significant conclusions with pol T7$^-$ and HIV-1 RT were that the bulk of the adduct at the O-6 atom had an inhibitory effect and that an inactive polymerase-oligonucleotide complex is in equilibrium with the functional form (16, 19).

Studies with pol T7$^-$ and HIV-1 RT indicated that the effect of size at the N-2 atom is more severe than at the O-6 atom (16,

* This work was supported in part by United States Public Health Service Grants R01 CA059887, R01 CA115309 (to L. A. P.), R01 ES010375, and P30 ES000267 (to F. P. G.). The costs of publication of this article were defrayed in part by the payment of page charges. This article must therefore be hereby marked "*advertisement*" in accordance with 18 U.S.C. Section 1734 solely to indicate this fact.

[S] The on-line version of this article (available at http://www.jbc.org) contains a MALDI-TOF mass spectrum and capillary gel electrophoresis analysis of the O^6-PobG 36-mer, an electrophoretic gel showing the lack of extension of an O^6-PobG:G mispair by pol η, and mass spectral analyses used to obtain the results shown in Fig. 7 (with the exception of data in Figs. 8–10 and Tables 3–5) and supplemental Figs. 1–13 and Tables 1–8.

[1] Both authors contributed equally to this work.

[2] Supported in part by a fellowship from Merck Research Laboratories.

[3] To whom correspondence should be addressed: Dept. of Biochemistry and Center in Molecular Toxicology, Vanderbilt University School of Medicine, 638 Robinson Research Bldg., 23rd and Pierce Aves., Nashville, TN 37232-0146. Tel.: 615-322-2261; Fax: 615-322-3141; E-mail: f.guengerich@vanderbilt.edu.

[4] The generic term "alkyl" is used to include both alkyl and aralkyl (Bz) groups for convenience.

[5] The abbreviations used are: Bz, benzyl; CID, collision-induced dissociation; dCTPαS, 2′-deoxycytidine 5′-*O*-(1-thiotriphosphate); DTT, dithiothreitol; ESI, electrospray ionization; LC-MS/MS, liquid chromatography-tandem mass spectrometry; MALDI-TOF, matrix-assisted laser desorption ionization/time-of-flight; MS, mass spectrometry; Pob, 4-oxo-4-(3-pyridyl)butyl; PCNA, proliferating cell nuclear antigen; pol, (DNA) polymerase; pol T7$^-$, bacteriophage pol T7 exonuclease-deficient; RT, reverse transcriptase; UDG, uracil DNA glycosylase; HIV-1, human immunodeficiency virus, type 1.

19, 20). However, these issues have not been addressed in detail with mammalian DNA polymerases, particularly replicative pol δ and the so-called translesion polymerases that bypass damage in cells (Y family, *e.g.* pol η, ι, and κ). We have systematically addressed the issue of the effect of bulk at the N-2 guanine atom on the insertion of dNTPs by several of the above polymerases (21–23), and we now apply similar quantitative approaches to O^6-alkylG adducts varying in size. The studies with O^6-MeG and O^6-BzG were extended to the larger adduct O^6-PobG, which is of relevance to tobacco-induced carcinogenesis (24–28). The O^6-PobG adduct is formed from the "tobacco-specific" carcinogen 4-(methylnitrosoamino)-1-(3-pyridyl)-1-butanone *in vivo* (27) and has been demonstrated to be mutagenic in both bacterial and mammalian cells (24, 25).

We found an effect of adduct size at the O-6 atom of G on activities of all the human DNA polymerases examined. The increase in adduct size resulted in attenuated steady-state k_{cat}/K_m parameters and a loss of the rapid burst phase in pre-steady-state analyses. The effects of the increased bulk varied with human polymerases pol δ, η, ι, and κ. Of these polymerases, pol η was clearly the most efficient in handling the bulkier lesions. O^6-PobG posed an almost complete block to pol δ. LC-MS/MS analysis of the pol η product of the O^6-BzG reaction indicated unexpected phenomena, −1 and −2 frameshifts and insertion of A, which may be relevant to complex phenomena observed previously in cells (24).

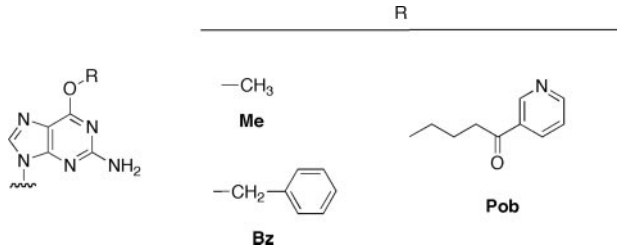

FIGURE 1. ***O*⁶-AlkylG derivatives studied in this work.**

TABLE 1
Oligonucleotides used in this study
G* indicates G, O^6-MeG, O^6-BzG, or O^6-PobG.

24-mer	5′–GCCTCGAGCCAGCCGCAGACGCAG
24-U-mer	5′–GCCUCGAGUCAGCCGUAGACGUAG
36-mer	3′–CGGAGCTCGGTCGGCGTCTGCGTC**G***CTCCTGCGGCT

EXPERIMENTAL PROCEDURES

Materials—Unlabeled dNTPs were obtained from Amersham Biosciences; S_p-dCTPαS was from Biolog Life Science Institute (Bremen, Germany), and [γ-^{32}P]ATP (specific activity 3×10^3 Ci mmol^{-1}) was from PerkinElmer Life Sciences. T4 polynucleotide kinase and restriction endonucleases were purchased from New England Biolabs (Beverly, MA). Bio-Spin columns were obtained from Bio-Rad. A protease inhibitor mixture (mixture) was from Roche Applied Science.

Oligonucleotides—The unmodified oligonucleotides and the O^6-MeG-modified 36-mer (Table 1) were purchased from Midland Certified Reagent Co. (Midland, TX). The 36-mer containing O^6-BzG was prepared using a modification of the procedure described elsewhere (16).

The 36-mer containing O^6-PobG was prepared from the phosphoramidite derivative (29) using slight modification of the procedure described elsewhere (16). The oligonucleotide was deprotected by stirring in 500 μl of concentrated NH_4OH at 55 °C for 12 h, filtered through a 0.45-μm filter, and neutralized to pH 7.4 with glacial CH_3CO_2H. The sample was desalted using an octadecylsilane (C_{18}) Sep-Pak column (Waters Associates, Milford, MA) and concentrated to dryness by lyophilization. Removal of the dithiane group was done using 300-fold excess *N*-chlorosuccinimide in 500 μl of 50% CH_3CN (v/v) at room temperature for 8 h. The oligonucleotide was purified by PAGE, extracted,

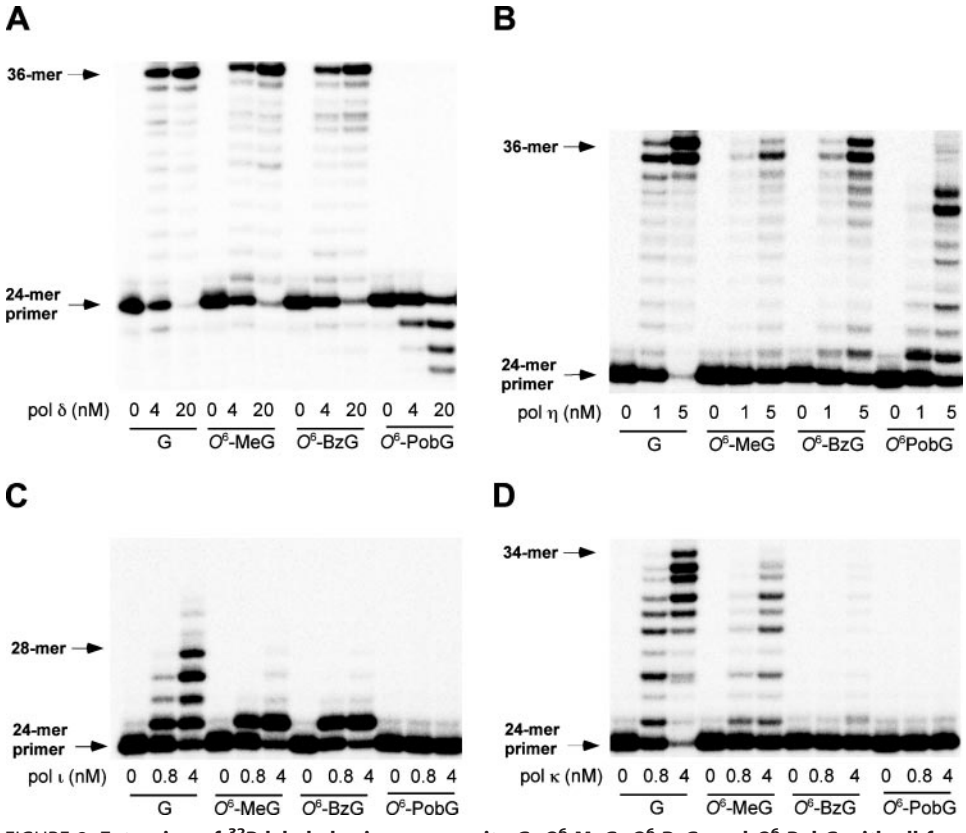

FIGURE 2. **Extension of ^{32}P-labeled primers opposite G, O^6-MeG, O^6-BzG, and O^6-PobG with all four dNTPs present.** *A*, pol δ; *B*, pol η; *C*, pol ι; *D*, pol κ. The primer (24-mer) was annealed with each of the four different 36-mer templates (Table 1) containing an unmodified G or O^6-modified G placed at the 25th position from the 3′-end. Reactions were done for 15 min with increasing concentrations of polymerases, as indicated, and 100 nM of DNA substrate (primer-template) as indicated. In the case of pol δ (*A*), 400 nM PCNA was also included (32). The ^{32}P-labeled 24-mer primer was extended in the presence of all four dNTPs. Reaction products were analyzed by denaturing gel electrophoresis with subsequent PhosphorImaging analysis. *A*, the degraded bands are attributed to the inherent exonuclease activity of pol δ.

TABLE 2
Steady-state kinetic parameters for 1-base incorporation by human pol δ, η, ι, and κ

Polymerase	Template	dNTP	K_m	k_{cat}	k_{cat}/K_m	f (misinsertion frequency)
			μM	s^{-1}	$mM^{-1}\ s^{-1}$	
pol δ/PCNA	G	C	0.049 ± 0.009	0.0096 ± 0.0001	196	1
		T	210 ± 20	0.022 ± 0.001	0.10	0.00051
	O^6-MeG	C	1.3 ± 0.3	0.021 ± 0.001	16	1
		T	1.3 ± 0.1	0.022 ± 0.001	17	1.0
	O^6-BzG	C	7.8 ± 0.9	0.016 ± 0.001	2.1	1
		T	8.1 ± 0.9	0.016 ± 0.001	2.0	0.95
pol η	G	C	2.6 ± 0.3	0.41 ± 0.01	160	1
		T	130 ± 20	0.15 ± 0.01	1.2	0.008
		A	98 ± 41	0.0021 ± 0.0002	0.02	0.0001
	O^6-MeG	C	8.7 ± 0.9	0.14 ± 0.01	16	1
		T	14 ± 3	0.20 ± 0.01	14	0.88
		A	84 ± 32	0.0027 ± 0.0002	0.03	0.0002
	O^6-BzG	C	51 ± 6	0.13 ± 0.01	2.5	1
		T	72 ± 11	0.22 ± 0.01	3.1	1.2
		A	61 ± 11	0.0021 ± 0.0001	0.03	0.01
	O^6-PobG	C	190 ± 20	0.12 ± 0.01	0.63	1
		G	77 ± 11	0.010 ± 0.001	0.13	0.21
		T	270 ± 50	0.0013 ± 0.0001	0.0048	0.008
		A	66 ± 18	0.0029 ± 0.0002	0.04	0.07
pol ι	G	C	88 ± 12	0.23 ± 0.01	2.6	1
		T	640 ± 60	0.30 ± 0.01	0.47	0.18
	O^6-MeG	C	360 ± 40	0.19 ± 0.01	0.53	1
		T	190 ± 30	1.0 ± 0.1	5.3	10
	O^6-BzG	C	260 ± 50	0.26 ± 0.02	1.0	1
		T	170 ± 20	0.57 ± 0.02	3.4	3.4
	O^6-PobG	C	400 ± 120	0.00021 ± 0.00003	0.0005	1
		G	94 ± 18	0.00044 ± 0.00002	0.0046	9.2
		T	82 ± 11	0.00068 ± 0.00002	0.0082	16
pol κ	G	C	8.4 ± 0.9	0.31 ± 0.01	36.9	1
		T	6800 ± 700	0.38 ± 0.02	0.056	0.0015
	O^6-MeG	C	790 ± 60	0.27 ± 0.01	0.34	1
		T	2400 ± 300	0.58 ± 0.04	0.24	0.71
	O^6-BzG	C	400 ± 70	0.016 ± 0.001	0.04	1
		T	1400 ± 100	0.031 ± 0.001	0.022	0.55
	O^6-PobG	C	2400 ± 300	0.0091 ± 0.0006	0.0037	1
		G	110 ± 20	0.00043 ± 0.00003	0.0039	1.1
		T	250 ± 70	0.000053 ± 0.000004	0.00021	0.057

desalted using a Sephadex G-10 column (Amersham Biosciences), and subsequently analyzed using MALDI-TOF MS and capillary gel electrophoresis (see Supplemental Material).

The extinction coefficients for the oligonucleotides, estimated by the Borer method (30), were as follow: 24-mer, ϵ_{260} = 224 $mM^{-1}\ cm^{-1}$; 25-mer, ϵ_{260} = 232 $mM^{-1}\ cm^{-1}$; and 36-mer, ϵ_{260} = 310 $mM^{-1}\ cm^{-1}$ (20, 21).

Expression and Purification of Human DNA Polymerases—Recombinant human pol δ (21, 31), pol η (21), pol ι (22), pol κ (23), and PCNA (32, 33) were prepared as described previously.

Reaction Conditions for Enzyme Assays—Standard DNA polymerase reactions were done in 50 mM Tris-HCl (pH 7.5) buffer containing 5 mM DTT, 100 μg of bovine serum albumin ml^{-1} (w/v), and 10% glycerol (v/v) with 100 nM primer-template at 37 °C (20–22), with 50 mM NaCl added in the experiments with pol η (21). Primers were 5′-end-labeled using T4 polynucleotide kinase/[γ-^{32}P]ATP and annealed with template (36-mer). All reactions were initiated by the addition of dNTP solutions containing $MgCl_2$ (5 mM final concentration) to preincubated enzyme/DNA mixtures.

Primer Extension Assay with All Four dNTPs ("Run-on" or "Standing Start" Experiments)—A ^{32}P-labeled primer, annealed to either an unmodified or modified (O^6-alkylG) template, was generally extended in the presence of all four dNTPs (100 μM each) for 15 min. In some cases (extension of A:O^6-alkylG mismatches), the dNTP concentrations were raised to 1 mM, and the incubation time was 60 min. Reaction mixtures (8 μl) were quenched with 2 volumes of a solution of 20 mM EDTA in 95% formamide (v/v) (20). Products were resolved using a 16% PAGE system (w/v) containing 8 M urea and visualized using a Molecular Imager FX and Quantity One software (Bio-Rad).

Steady-state Kinetic Analyses—A ^{32}P-labeled primer, annealed to either an unmodified or adducted template, was extended in the presence of varying concentrations of a single dNTP. The molar ratio of primer-template complex to enzyme was at least 10:1. Polymerase concentrations and reaction times were chosen so that maximal product formation was ≤20% of the substrate concentration (34). The primer-template complex was extended with dNTP in the presence of 0.1–5 nM enzyme for 5–30 min. All reactions (8 μl) were done at ≥10 dNTP concentrations (in duplicate) and quenched with 2 vol-

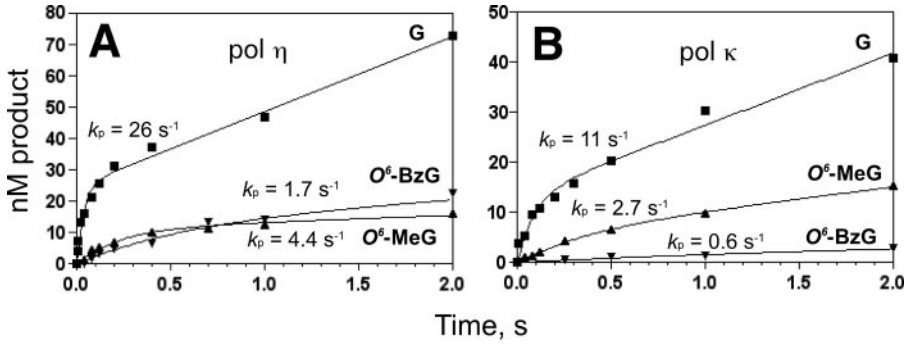

FIGURE 3. **Pre-steady-state burst kinetics of incorporation opposite G, O^6-MeG, and O^6-BzG by human pols η and κ.** *A*, pol η; *B*, pol κ. pol η or κ (25 and 17 nM, respectively) was incubated with 100 nM 24-mer/36-mer primer-template complex in a rapid quench-flow instrument and mixed with dCTP (and $MgCl_2$) to initiate reactions as follows: 1 mM dCTP for the 24-mer/36-G-mer (■), 24-mer/36-O^6-MeG-mer (▲), and 24-mer/36-O^6-BzG-mer (▼). The polymerization reactions were quenched with 0.3 M EDTA at the indicated time intervals, and product formation was determined following gel electrophoresis separation and PhosphorImaging. The data were fit to the following burst equation: $y = A(1 - e^{-kpt}) + k_{ss}t$, as described under "Experimental Procedures" (without normalization of k_{ss} for enzyme concentration in the equation). Pre-steady-state rates (k_p) were estimated for pol η as follows: G-mer, $k_p = 26.3 \pm 4.8\ s^{-1}$ and $k_{ss} = 0.95 \pm 0.06\ s^{-1}$; O^6-MeG-mer, $k_p = 4.4 \pm 0.7\ s^{-1}$ and $k_{ss} = 0.088 \pm 0.006\ s^{-1}$; O^6-BzG-mer, $k_p = 1.7 \pm 0.1\ s^{-1}$ and $k_{ss} = 0.16 \pm 0.01\ s^{-1}$. For pol κ the values were as follows: G-mer, $k_p = 11 \pm 3\ s^{-1}$ and $k_{ss} = 0.85 \pm 0.08\ s^{-1}$; O^6-MeG-mer, $k_p = 2.7 \pm 0.4\ s^{-1}$ and $k_{ss} = 0.27 \pm 0.01\ s^{-1}$; O^6-BzG-mer, $k_p = 0.6 \pm 0.3\ s^{-1}$ and $k_{ss} = 0.034 \pm 0.007\ s^{-1}$.

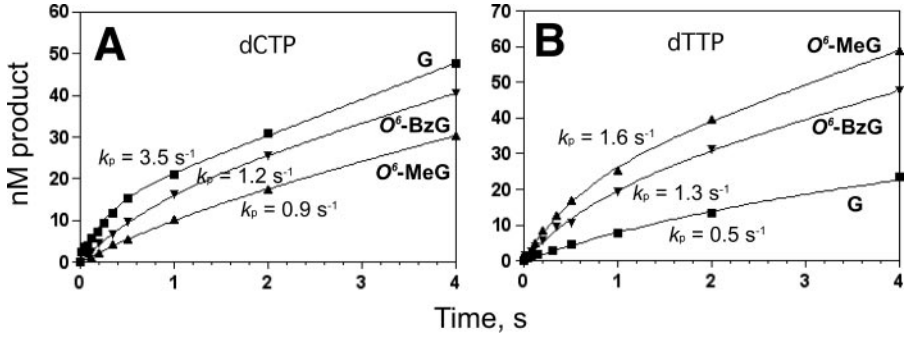

FIGURE 4. **Pre-steady-state kinetic analysis of incorporation of dCTP and dTTP opposite G, O^6-MeG, and O^6-BzG by human pol ι.** *A*, dCTP incorporation; *B*, dTTP incorporation. pol ι (24 nM) was incubated with 100 nM 24-mer/36-mer primer-template complex in a rapid quench-flow instrument and mixed with 1 mM dCTP or dTTP (and $MgCl_2$) to initiate reactions as follows: 24-mer/36-G-mer (■), 24-mer/36-O^6-MeG-mer (▲), and 24-mer/36-O^6-BzG-mer (▼). The polymerization reactions were quenched with 0.3 M EDTA at the indicated time intervals, and product formation was determined following separation by gel electrophoresis and PhosphorImaging. The data were fit to the following burst equation: $y = A(1 - e^{-kpt}) + k_{ss}t$, as described under "Experimental Procedures" (without normalization of k_{ss} for enzyme concentration in the equation). Pre-steady-state rates (k_p) were estimated for dCTP as follows: G-mer, $k_p = 3.5 \pm 0.5\ s^{-1}$ and $k_{ss} = 0.36 \pm 0.02\ s^{-1}$; O^6-MeG-mer, $k_p = 0.9 \pm 0.3\ s^{-1}$ and $k_{ss} = 0.25 \pm 0.03\ s^{-1}$; O^6-BzG-mer, $k_p = 1.2 \pm 0.2\ s^{-1}$ and $k_{ss} = 0.29 \pm 0.01\ s^{-1}$. With dTTP the values were as follows: G-mer, $k_p = 0.5 \pm 0.1\ s^{-1}$ and $k_{ss} = 0.11 \pm 0.01\ s^{-1}$; O^6-MeG-mer, $k_p = 1.6 \pm 0.2\ s^{-1}$ and $k_{ss} = 0.4 \pm 0.03\ s^{-1}$; O^6-BzG-mer, $k_p = 1.3 \pm 0.3\ s^{-1}$ and $k_{ss} = 0.33 \pm 0.04\ s^{-1}$.

umes of a solution of 20 mM EDTA in 95% formamide (v/v) (20–22). Products were resolved using 16% polyacrylamide gels (w/v) containing 8 M urea and quantitated with PhosphorImaging analysis using a Molecular Imager FX instrument and Quantity One software (Bio-Rad). Graphs of product formation *versus* dNTP concentration were fit using nonlinear regression (hyperbolic fits) in GraphPad Prism version 3.0 (San Diego, CA) for the determination of k_{cat} and K_m values.

Pre-steady-state Reactions—Rapid quench experiments were performed using a model RQF-3 KinTek Quench Flow Apparatus (KinTek Corp., Austin, TX). Reactions were initiated by rapid mixing of ^{32}P-primer-template/polymerase mixtures (12.5 μl) with the dNTP-Mg^{2+} complex (10.9 μl) and then quenched with 0.3 M EDTA after reaction times varying from 5 ms to 4 s with G in the template (or 8 s for O^6-MeG- and O^6-BzG-, or 30 s for O^6-PobG-containing DNA) (21–23). Reaction products were mixed with 450 μl of a formamide/dye solution (20 mM EDTA, 95% formamide (v/v), 0.5% bromphenol blue (w/v), and 0.05% xylene cyanol (w/v)) and separated using denaturing electrophoresis gels, with quantitation as described for the steady-state reactions. Pre-steady-state data points were fit to the following burst equation: $y = A(1 - e^{-kpt}) + k_{ss}t$, whereas y indicates the concentration of product; A indicates the burst amplitude; k_p indicates the pre-steady-state rate of nucleotide incorporation; t indicates time, and k_{ss} indicates the steady-state rate of nucleotide incorporation (not normalized for enzyme concentration in the equation) (35, 36), using nonlinear regression analysis in GraphPad Prism version 3.0.

Phosphorothioate Analysis—With the ^{32}P-primer annealed to either an unmodified or adducted template, reactions were initiated by rapid mixing of ^{32}P-primer-template/polymerase mixtures (12.5 μl) with S_p-dCTPαS-Mg^{2+} complex (or dCTP-Mg^{2+}) (10.9 μl) and then quenched with 0.3 M EDTA after reaction times varying from 5 ms to 30 s for O^6-PobG-containing DNA. Products were analyzed as described for the pre-steady-state reactions (see above).

LC-MS/MS Analysis of Oligonucleotide Products from pol η Reactions—In a typical reaction, 1–4 nmol of DNA (primer-template) and 50–100 pmol of pol η were mixed in 50 mM Tris-HCl buffer (pH 7.7) containing 2 mM DTT, 50 mM NaCl, 5 mM $MgCl_2$, and 100 μg of bovine serum albumin ml^{-1} in a total volume of 100 μl. The reaction was initiated by adding 1 mM each of four dNTPs and incubated for 4 h at 37 °C. The reaction was terminated by removal of the excess dNTPs using a spin column (Bio-Spin 6 chromatography column, Bio-Rad). To the above filtrate (~100 μl), Tris-HCl buffer (50 mM), DTT (2 mM), and UDG (6 units) were added, and the volume was made up to 200 μl (37). The reaction mixture was incubated for 5 h at 37 °C, then heated at 95 °C for 1 h in the presence of 0.5 M piperidine, and finally concentrated to dryness by lyophilization; the residue was dissolved in 100 μl of H_2O for LC-MS/MS analysis.

LC-MS/MS was performed on an Acquity ultraperformance liquid chromatography system (Waters Associates) connected to a Finnigan LTQ mass spectrometer (ThermoElectron Corp., San Jose, CA), operating in the ESI negative ion mode and using

an Acquity ultraperformance liquid chromatography system BEH octadecylsilane (C_{18}) column (1.7 μm, 1.0 × 100 mm). LC conditions were as follows: buffer A contained 10 mM $NH_4CH_3CO_2$ plus 2% CH_3CN (v/v), and buffer B contained 10 mM $NH_4CH_3CO_2$ plus 95% CH_3CN (v/v). The following gradient program was used with a flow rate of 150 μl min^{-1}: 0–3 min, linear gradient from 100% A to 97% A/3% B (v/v); 3–4.5 min, linear gradient to 80% A/20% B (v/v); 4.5–5 min, linear gradient to 100% B; 5–5.5 min, hold at 100% B; 5.5–6.5 min, linear gradient to 100% A; 6.5–9.5 min, hold at 100% A. The temperature of the column was maintained at 50 °C. Samples (10 μl) were infused with an autosampler system. ESI conditions were as follows: source voltage 4 kV, source current 100 μA, auxiliary gas flow rate setting 20, sweep gas flow rate setting 5, sheath gas flow setting 34, capillary voltage −49 V, capillary temperature 350 °C, tube lens voltage −90 V. MS/MS conditions were as follows: normalized collision energy 35%, activation *Q* 0.250, and activation time 30 ms. Product ion spectra were acquired over the range *m/z* 300–2000. The triply (negatively) charged species were generally used for CID analysis; in some cases the −4 ions were used. The calculations of the CID fragmentations of oligonucleotide sequences were done using a program linked to the Mass Spectrometry Group of Medicinal Chemistry at the University of Utah (38).

RESULTS

Overall Strategy—As in previous work with the two replicative viral polymerases HIV-1 RT and pol T7⁻ (16, 19), comparisons were made with the four human DNA polymerases (δ, η, ι, and κ) with Me and Bz substituents at the O-6 atom of G. In addition, an even larger adduct of direct relevance to tobacco-induced carcinogenesis, O^6-PobG, was included in comparisons. Initial studies involved extension of a 24-mer primer opposite templates containing each of the adducts, followed by more quantitative steady-state kinetic analysis of the insertion reactions. Further analysis involved pre-steady-state kinetic measurements of incorporation with three of the polymerases (η, ι, and κ). The most active polymerase with all three O^6-alkylG adducts (pol η) was analyzed to characterize all the products.

Primer Extension Past O^6-AlkylG Adducts Using All Four dNTPs—Preliminary studies indicated that pol δ activity is stimulated by the presence of PCNA. None of the other polymerases were stimulated by the addition of PCNA under these conditions, without or with these or any of several other DNA adducts (21–23). pol δ readily extended the primer opposite the O^6-MeG and O^6-BzG templates but was completely blocked by O^6-PobG, and exonuclease activity was seen in the latter case (Fig. 2*A*). pol η was hindered by all of the O^6-alkylG adducts but nevertheless extended all three (Fig. 2*B*). The product derived from the primer opposite O^6-PobG appeared not to be full-length, and the analysis is considered later in this work. pol ι showed considerable 1-base incorporation opposite O^6-MeG and O^6-BzG but little opposite O^6-PobG (Fig. 2*C*). pol κ showed limited 1-base incorporation and extension beyond O^6-MeG and O^6-BzG but very little activity with O^6-PobG (Fig. 2*D*).

Steady-state Kinetics of dNTP Incorporation Opposite G and O^6-AlkylG Adducts—Preliminary analyses with individual dNTPs showed that, as with processive polymerases (16, 39), mainly C or T was incorporated opposite O^6-MeG and O^6-BzG. With O^6-PobG, some dGTP incorporation also occurred, and incorporation was subsequently measured with all four dNTPs with pol η. Rates of incorporation of dATP by pol η were also measured for all three adducts because of results obtained later in the work (see below). Rates were measured as a function of the concentration of each dNTP, and the steady-state kinetic parameters were determined (Table 2).

The most meaningful parameters in this work are k_{cat}/K_m, the catalytic specificity, and *f*, the misinsertion frequency, which is based on the ratio of insertion of the incorrect dNTP to that of dCTP (40). pol δ, η, and κ showed similar incorporation efficiencies for dCTP and dTTP with both O^6-MeG and O^6-BzG, similar to the case of HIV-1 RT (16). pol ι inserted T in preference to C, by an order of magnitude, similar to the case of pol T7⁻, for both O^6-MeG and O^6-BzG (16).

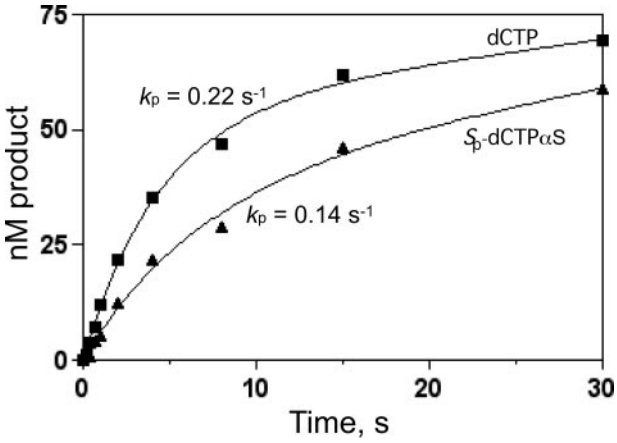

FIGURE 5. **Phosphorothioate analysis of pre-steady-state kinetics of dCTP incorporation opposite O^6-PobG by human pol η.** pol η (50 nM) was incubated with 100 nM 24-mer/36-mer primer-template complexes (^{32}P-labeled primer) in a rapid quench-flow instrument and mixed with 1 mM dCTP (■) or S_p-dCTPαS (▲) to initiate reactions for the 24-mer/36-O^6-PobG-mer. The following rates were estimated: dCTP, k_p = 0.22 ± 0.03 s^{-1}; S_p-dCTPαS, k_p = 0.14 ± 0.05 s^{-1}.

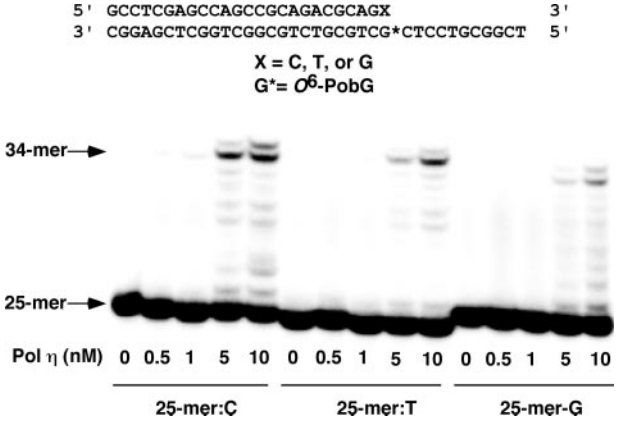

FIGURE 6. **Extension of primers with C, T, or G positioned opposite O^6-PobG by pol η.** Primer (24-mer, Table 1, with an additional C, T, or G at the 3′-end) was annealed to 36-mer template (Table 1) containing an O^6-PobG placed at the 25th position from the 3′-end. Reactions were done for 15 min with increasing concentrations of pol η, as indicated, and 100 nM of DNA substrate (primer-template) as indicated. The ^{32}P-labeled primers were extended in the presence of all four dNTPs. Reaction products were analyzed by denaturing gel electrophoresis with subsequent PhosphorImaging analysis.

With O^6-PobG in the template, dGTP was also incorporated. The order of preference of individual dNTPs varied among the polymerases, showing the order (based on k_{cat}/K_m) C > G > A > T for pol η, T > G > C for pol ι, and C ~ G > T for pol κ. The k_{cat}/K_m for dCTP incorporation opposite O^6-PobG by pol η is considerably less than for O^6-MeG or O^6-BzG by the same enzyme but still much higher than for incorporation of any dNTPs opposite this adduct by any of the other polymerases.

O⁶-MeG	C	GAGGACGCCG	23 %
	T	GAGGACGCCG	50 %
	T	GAGGACGCC	27 %
O⁶-PobG	C	GAGGACGCCGA	19 %
	C	GAGGACGCCG	59 %
	T	GAGGACGCCG	20 %
	T	GAGGACGCC	2 %
O⁶-BzG		AGGACGCCGA	1 %
		GAGGACGCCGA	2 %
	C	GAGGACGCCGA	37 %
	C	GAGGACGCCGAA	13 %
	C	GAGGACGCCGAG	5 %
	T	GAGGACGCCGA	23 %
	T	GAGGACGCCGAA	8 %
	A	GAGGACGCCGA	11 %

5' GCCUCGAGUCAGCCGUAGACGUAG
3' CGGAGCTCGGTCGGCGTCTGCGTCG*CTCCTGCGGCT

FIGURE 7. **Products of extension of O^6-alkylG template-primer complexes by pol η.** Data used to derive these results are presented in Figs. 8–10 and Tables 3–5 and in the Supplemental Material (supplemental Figs. S3–S13 and Tables S1–S8).

Pre-steady-state Burst Kinetics of dNTP Incorporation Opposite G and O^6-AlkylG Adducts—Steady-state kinetic parameters are useful in understanding DNA polymerases but are limited in the amount of information they can provide in terms of mechanistic details about catalysis (41). To our knowledge, pre-steady-state kinetic measurements have not been reported previously for any of these enzymes with O^6-alkylG substrates.

As expected from the results of studies with other oligonucleotide sequences, kinetic bursts were observed with pol η, ι, and κ for insertion of dCTP opposite G (Figs. 3 and 4) (21–23). These results indicate that a step in catalysis occurring *after* product formation is at least partially rate-limiting (42). The bursts seen with pol ι (Fig. 4) do not break as sharply as with pol η and pol κ (Fig. 3), probably because of the slower k_p. (The

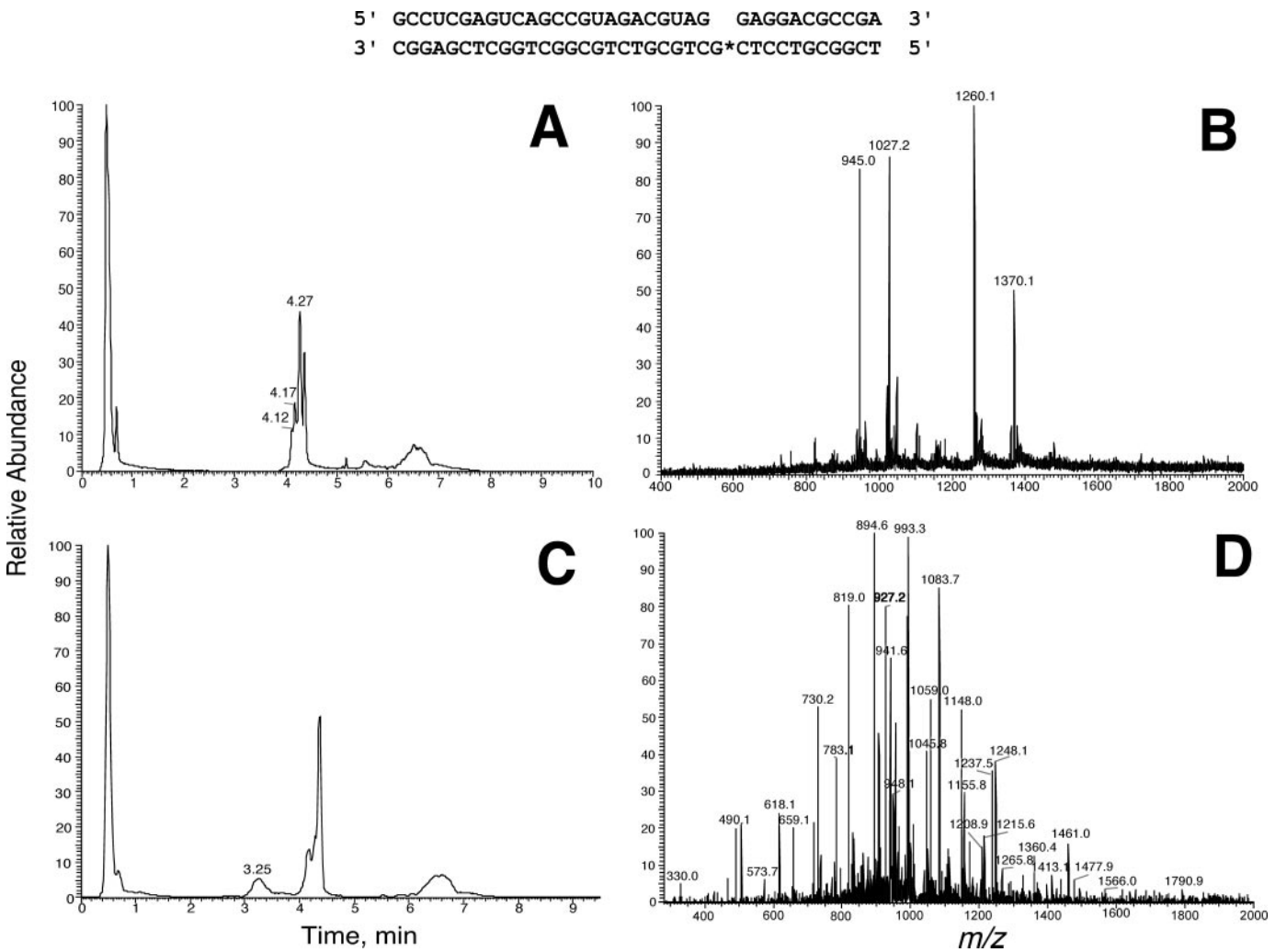

FIGURE 8. **LC-MS/MS analysis of the pol −1 deletion product of extension of the primer opposite the template containing O^6-BzG.** The reaction mixture containing the oligonucleotide fragments obtained by UDG hydrolysis. *A*, total ion current trace of the extension products. *B*, ESI mass spectrum of the peaks eluted at 3.25 min in *A*. *C*, reconstructed single reaction monitoring profile of *m/z* 1027.2. *D*, CID spectrum of *m/z* 1027.2. See Table 3 for lists of assignments of CID ions. The *m/z* 945.0 and 1260.1 ions are the −4 and −3 charged species, respectively, resulting from the same product (−2 deletion product; supplemental Fig. S10); the *m/z* 1027.2 and 1370.1 ions are the −4 and −3 charged species, respectively, resulting from another product, namely the one used for the CID (*D*) and shown with the sequence at the *top* of the figure.

amount of pol δ available was not sufficient to conduct these experiments.)

Some burst character was retained when the experiments were repeated with O^6-MeG in the cases of pol η and κ (Fig. 3). With O^6-BzG the bursts were largely abolished. The loss of the burst is interpreted to mean that a step occurring prior to the formation of product (presumably phosphodiester bond formation or possibly a conformational step) is now slower than product release. With pol ι (Fig. 4), the trend in the kinetics was G > O^6-BzG > O^6-MeG (Fig. 4*A*), which was unexpected. An opposite pattern was seen for dTTP incorporation with pol ι, which is very error-prone with these lesions (Table 1), and only a semblance of a burst was observed with both O^6-MeG and O^6-BzG (Fig. 4*B*).

Phosphorothioate Analysis of dCTP Incorporation Opposite O^6-PobG by pol η—One approach to further delineate aspects of catalysis by DNA polymerases is the use of sulfur *versus* oxygen elemental ("thio") effects on rates. The principle is similar to that utilized with kinetic isotope effects, in that the substitution of an α-oxygen of a dNTP with sulfur decreases the electronegativity and makes bond breakage more difficult. If this is a slow step in the reaction, then the overall reaction will be slowed (43, 44). This is a simplistic interpretation and, as with many aspects of kinetic hydrogen isotope effects, the detailed interpretation of the extent of the changes has some differences in opinion (43, 45, 46).

pol η was studied in the context of an elemental effect for incorporation of dCTP opposite O^6-PobG, in that this is the most active of the polymerases studied here with this adduct. The elemental effect on the early incorporation phase was only ~1.5 (Fig. 5), only slightly higher than reported for incorporation of dCTP opposite G with this enzyme (21).

pol η Extension beyond O^6-AlkylG Paired with Bases—Of the human DNA polymerases examined, pol δ and pol η were the most catalytically efficient in incorporating dNTPs opposite the O^6-MeG and O^6-BzG adducts (Table 2). pol η was the only polymerase that could incorporate opposite O^6-PobG with appreciable efficiency (Table 2) and extend the product (Fig. 2). pol η inserted C, T, and G (Table 2), but this information by itself may not predict the outcome of subsequent extension steps. To address the issue, we prepared primers with either C, T, or G positioned opposite O^6-PobG and used varying concentrations of pol η in the presence of all four dNTPs (Fig. 6). The primers with the pyrimidines (C, T) positioned opposite O^6-PobG were extended; with G the extension was much slower. The results suggest that when G is inserted, it is positioned opposite the C 5′ of the O^6-PobG in the sequence and that the resulting distortion is not favorable for extension by pol η.

In the work with pol η, we also detected some incorporation of A opposite each of the three O^6-alkylG adducts (Table 2). The catalytic efficiency was low and roughly similar with each adduct. To determine whether these products (with A positioned opposite O^6-alkylG adducts) are extended, we prepared the (radiolabeled) primers with the A at the 3′ position and incubated with varying concentrations of pol η in the presence of all four dNTPs. The results showed very limited extension of primers having an A paired with any of the three O^6-alkylG lesions studied here, particularly O^6-PobG (supplemental Fig. S2).

TABLE 3

Observed and theoretical CID fragmentation for pol η − 1 deletion product with O^6-BzG

The assigned sequence was 5′-pAGGAGGACGCCGA-3′ (Fig. 8). See Ref. 53 for nomenclature of fragments.

Fragment assignment	Observed	Theoretical
5′-pA (a_2-B)	490.1	490.1
5′-pAG (a_3-B)	819.0	819.1
5′-pAGG (a_4-B)	1148.0	1148.2
5′-pAGGA (a_5-B)	1461.0	1461.2
(a_5-B, −2)	730.2	730.1
5′-pAGGAG (a_6-B)	1790.9	1790.3
(a_6-B, −2)	894.6	894.6
5′-pAGGAGG (a_7-B, −2)	1059.0	1059.2
5′-pAGGAGGA (a_8-B, −2)	1215.6	1215.7
5′-pAGGAGGAC (a_9-B, −2)	1360.4	1360.2
(a_9-B, −3)	906.4	906.5
5′-pAGGAGGACGCC (a_{12}-B, −3)	1208.9	1208.8
pGGAGGACGCCGA-3′ (w_{12}, −3)	1268.8	1265.2
pGAGGACGCCGA-3′ (w_{11}, −3)	1155.8	1155.5
pAGGACGCCGA-3′ (w_{10}, −3)	1045.8	1045.8
pGGACGCCGA-3′ (w_9, −2)	1413.1	1412.7
(w_9, −3)	941.8	941.5
pGACGCCGA-3′ (w_8, −2)	1248.1	1248.2
pACGCCGA-3′ (w_7, −2)	1083.7	1083.7
pCGCCGA-3′ (w_6, −2)	927.2	927.1
pGCCGA-3′ (w_5, −1)	1566.0	1566.3
(w_5, −2)	782.5	782.6
pCCGA-3′ (w_4, −1)	1237.0	1237.2
pCGA-3′ (w_3, −1)	948.1	948.2
pGA-3′ (w_2, −1)	659.1	659.1
pA-3′ (w_1, −1)	330.0	330.1

Analysis of Primer Incorporation/Extension Products Using LC-MS/MS with pol η Extension Products—To understand misincorporation and mutational events, it is desirable to determine the effects of modified DNA templates on the outcome of multiple primer incorporation events, which have not been specifically addressed in the experiments presented thus far in this paper. Many of the events involve incorporation of a single dNTP (Table 2 and Figs. 3–5) or multiple incorporation (extension events in which the products are not characterized) (Figs. 2 and 6). We utilized an approach to the sequence analysis of oligonucleotides using LC-MS/MS (47), which has been modified for this work. A key element for the success of this method is the placement of uracil residues in the primer strand and the use of UDG to then reduce the size of the product to facilitate sequence analysis with LC-MS/MS (37).

The analysis of the extension products of the primer opposite the O^6-alkylG lesions presented a technical challenge, in that complex mixtures of products were obtained even when a high concentration of pol η was used (50 pmol (not shown), *cf.* 4–10 pmol in Figs. 2 and 6), and the concentration of dNTPs was raised to 1 mM each in these assays. pol η has a tendency to stop just short of the terminus of the primer-template complex, at least part of the time, but can also add residues at the end in "blunt-end" additions. Thus, discerning whether the shorter lengths of products is because of frameshifts or to stopping at the end of the primer was not possible without sequence analysis.

The results of the pol η experiments with the three templates are shown in Fig. 7. For O^6-MeG and O^6-PobG, all of the detected products resulted from insertion of C (correct) or T opposite the modified G. With O^6-MeG, 77% of the products

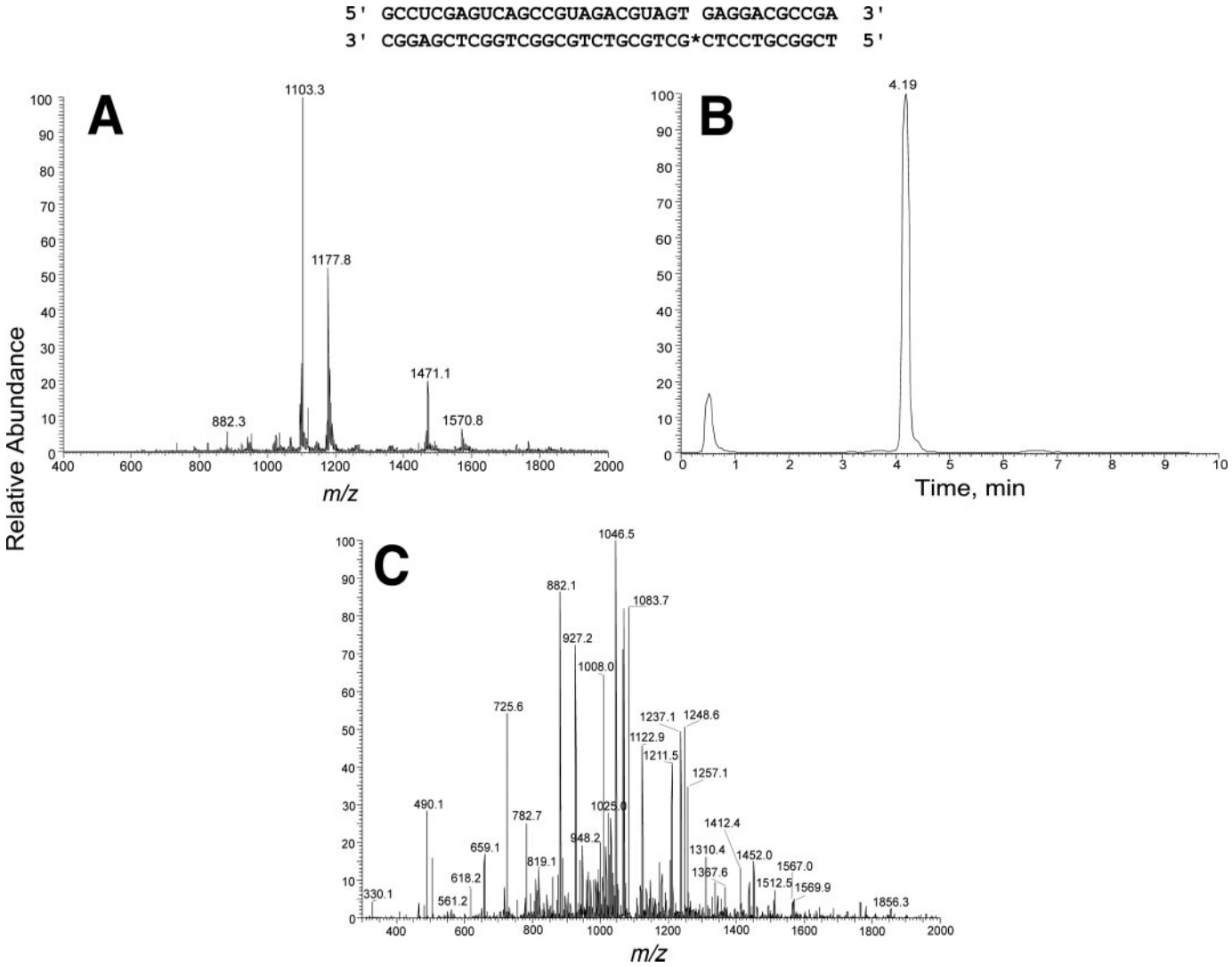

FIGURE 9. **LC-MS/MS analysis of the pol η T insertion product of extension of the primer opposite the template containing O^6-BzG.** The reaction mixture containing the oligonucleotide fragments obtained by UDG hydrolysis. The total ion current trace is shown in Fig. 8*A*. *A*, ESI mass spectrum of the peaks eluted at 4.19 min in Fig. 8*A*. *B*, reconstructed single reaction monitoring profile of *m/z* 1103.3. *C*, CID spectrum of *m/z* 1103.3. See Table 4 for lists of assignments of CID ions.

resulted from T insertion (23% C), and with O^6-PobG the combined T insertion products accounted for 22% of the products (78% C). The lengths of the products of the O^6-MeG products, and to some extent the O^6-PobG products, were slightly shorter than in the case of the O^6-BzG products (Fig. 7) (in apparent contrast to the gel results shown in Fig. 2, although the conditions used in the experiments in Fig. 2 were not as prolonged). None of the products contained a G inserted opposite the O^6-PobG.

With primer extension opposite O^6-BzG, the products obtained were much more complex than suggested by the gels (Figs. 2 and 6). Since we began using this analytical method (37, 48–52), the mixture of eight oligonucleotides is the most complex we have seen to date. With the present equipment available, this mixture could be readily analyzed, even if some of the products were present at only the 1–2% level.

LC-MS/MS analysis indicated the presence of eight products (Fig. 8). Initial LC showed a complex mixture including proteins and reagents with the oligonucleotides eluting at $t_R \sim 4$ min (with an additional oligonucleotide subsequently found at t_R 3.25 min) (Fig. 8*A*). The mass spectra showed seven peaks at *m/z* 945.0, 1027.2, 1099.6, 1103.3, 1105.5, 1177.8, and 1181.9, which are apparently the −4 charge ions (Fig. 8*B*) (subsequent work showed that the *m/z* 1181.9 peak was because of two separate products; see supplemental Fig. S11). A reconstructed trace of the *m/z* 1027.2 ion is shown in Fig. 8*C*. CID of the *m/z* 1027.2 ion (product eluted at t_R 3.25 min) produced the fragments shown in Fig. 8*D*. Inspection of these with the sequences of possible products (38) led to the assignment of the sequence as that shown at the top of Fig. 8 (Table 3) with a −1 deletion following O^6-BzG, followed then by error-free polymerization until the end (yielding a net −1 frameshift) (Figs. 7 and 8). Integration of the reconstructed ion chromatograms for the −4 ions led to the assignment of relative yields for the products identified in Figs. 7 and 8*B*, assuming equal ionization, and the products were identified using CID analysis (Figs. 7–10; supplemental Figs. S3–S13; Tables 3–5; and supplemental Tables S1–S8). The main product (37%) resulted from error-free

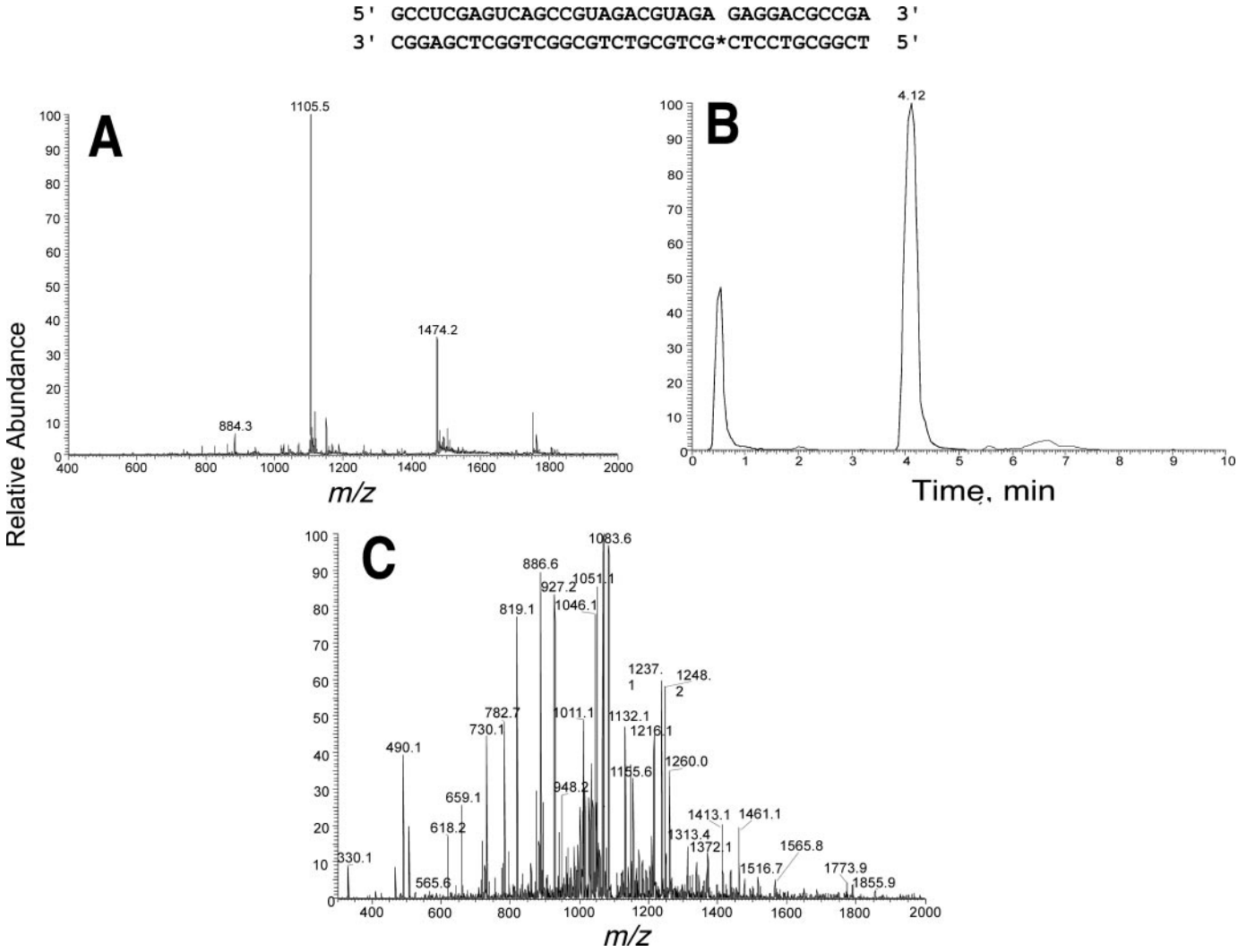

FIGURE 10. **LC-MS/MS analysis of the pol η A misinsertion product of extension of the primer opposite the template containing O^6-BzG.** The reaction mixture containing the oligonucleotide fragments obtained by UDG hydrolysis. The total ion current trace is shown in Fig. 8*A*. *A*, ESI mass spectrum of the peaks eluted at 4.12 min in Fig. 8*A*. *B*, reconstructed single reaction monitoring profile of *m/z* 1105.5. *C*, CID spectrum of *m/z* 1105.5. See Table 5 for lists of assignments of CID ions.

polymerization. Two products with T inserted opposite O^6-BzG were obtained (total of 31%), with one including a blunt-end A addition at the end (Fig. 9). Another product, with A inserted opposite O^6-BzG, accounted for 11% of the total product (Fig. 10). Accurate polymerization occurred after insertion of T; one product stopped 1 base short of the end and the other (minor) 2 bases short (Fig. 9).

DISCUSSION

Many studies have dealt with the misincorporation of nucleoside triphosphates opposite O^6-alkylG residues, which are among the most mutagenic of modifications of DNA by alkylating agents (5, 6, 54). O^6-MeG was the first lesion to be studied using the approach of site-specific mutagenesis (in bacterial systems) (8). Despite the interest in O^6-alkylG lesions and their mutagenicity, only limited information is available about mammalian DNA polymerases involved in the replication of O^6-alkylG lesions. O^6-MeG is an important lesion that is generated from many methylating agents, and even animals that have not been treated contain a finite amount of the adduct (presumably derived from *S*-adenosylmethionine (55)). Both O^6-MeG and O^6-PobG can be derived from the tobacco-specific nitrosamine 4-(methylnitrosoamino)-1-(3-pyridyl)-1-butanone (27). O^6-BzG is not apparently an environmental issue but has been used extensively as a model in previous work (9–12, 16, 19).

Several of the major DNA polymerases were examined, using recombinant preparations. Of these, only pol δ has shown a requirement for the presence of PCNA in copying past DNA adducts on relatively short oligonucleotides (32, 56); pol δ copied reasonably well past O^6-MeG and O^6-BzG but was completely blocked by O^6-PobG (Fig. 2). The translesion polymerases pol ι and κ could insert C and T opposite the O^6-alkylG adducts but, except in the case of pol κ with O^6-MeG, were not very efficient in extending the initial product.

pol η was the most efficient of these enzymes in processing all three of the O^6-alkylG residues (Fig. 1 and Table 2). Both the steady-state kinetic estimates of catalytic efficiency (single-base incorporation) and LC-MS/MS sequence analyses of the

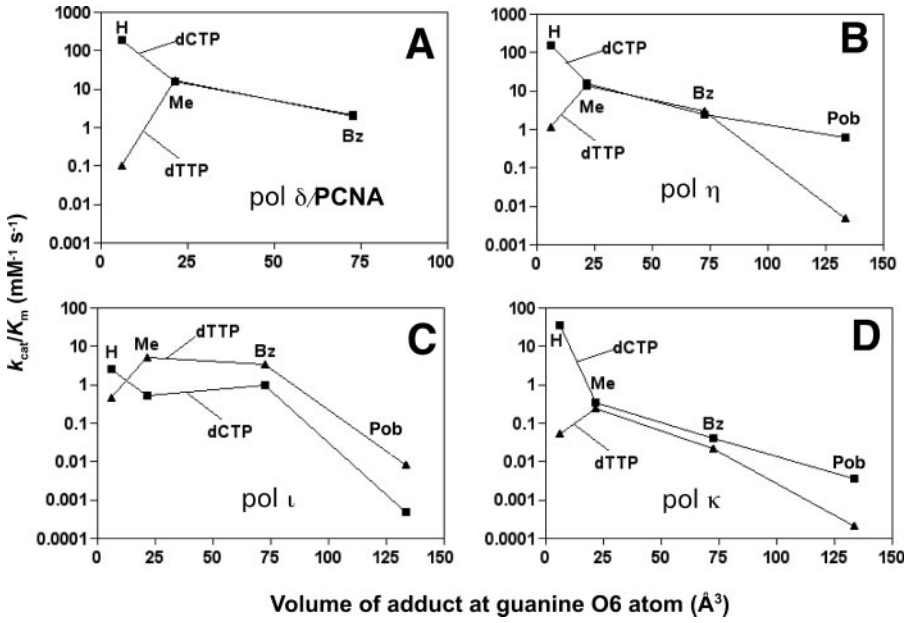

FIGURE 11. **Catalytic efficiency (k_{cat}/K_m) for dCTP incorporation opposite O^6-alkylG adducts by human polymerases as a function of the calculated volume of the adduct at the guanine O-6 atom.** Molecular volumes (Å^3) of adducts at the guanine O-6 atom were calculated using the program Chem3D (version 7.0), based on the Connolly surface algorithm (57), and plotted against k_{cat}/K_m values (Table 2) for dCTP (■) and dTTP (▲) incorporation for various O^6-alkylG adducts by the four human polymerases. *A*, pol δ (PCNA complex); *B*, pol η; *C*, pol ι; *D*, pol κ.

extended products show incorporation of C opposite the O^6-alkylG adducts, with a substantial incorporation of T (Table 2 and Fig. 9). G could be inserted opposite O^6-PobG but not efficiently extended (Table 2 and Fig. 6). In the case of O^6-BzG, but not with O^6-MeG or O^6-PobG, the LC-MS/MS analysis also revealed a product with A inserted (opposite O^6-BzG) and then accurately extended and small amounts of −1 and −2 deletion products (Fig. 7). Under the conditions used here, the LC-MS/MS analysis (Fig. 7) was more sensitive in detecting minor events, *e.g.* incorporation and extension of A opposite O^6-BzG, than were the ^{32}P-gel assays (Table 2 and supplemental Fig. S2).

One approach to analyzing the effects of different chemical adducts at a given site on DNA is to compare a quantitative parameter, *e.g.* the apparent catalytic efficiency k_{cat}/K_m, as a function of molecular properties, *e.g.* size. This approach, which has been done with all of these polymerases and N^2-alkylG adducts (21–23), has two caveats as follows: (i) the k_{cat}/K_m value is a relatively crude parameter of true enzyme efficiency, in that steady-state kinetic parameters can be misleading with DNA polymerases (41); and (ii) varying the size of the substituent (at the O-6 atom) results in a change of not only the steric bulk but also the hydrophobicity and electronic properties. However, the information is still of use in understanding how different DNA polymerases respond to various DNA modifications (21–23). With all of the four human DNA polymerases examined (Fig. 11), the addition of a Me group at the O-6 atom lowered the efficiency of dCTP insertion *and* also enhanced the insertion of dTTP, both by 1 order of magnitude. This general *enhancement* of insertion of a wrong dNTP because of modification is usually not seen with other DNA adducts (21–23) (the stimulatory effect of O^6 methylation on dTTP insertion was also seen with pol T7$^-$ and HIV-1 RT (16)).

In the analysis of the effect of O^6-PobG in the log (k_{cat}/K_m) *versus* size relationship (Fig. 11), the size effect (discounting any other contributors) on C and T incorporation follows a pattern for pol κ but is much more severe for pol ι. With pol η there is a "linear" drop in the efficiency of dCTP incorporation but a more precipitous drop in the efficiency of dTTP incorporation. The overall result is an apparently higher fidelity index (lower misincorporation frequency, *f*) for misincorporation opposite an O^6-PobG adduct compared with O^6-MeG and O^6-BzG (Fig. 11 and Table 2). The LC-MS/MS analysis of primer extension products (Fig. 7) also showed a higher frequency of correct insertion products for O^6-PobG than O^6-MeG or O^6-BzG.

The size effects (Fig. 11) can be compared with those reported with N^2-alkylG and N^2-aralkylG adducts with these polymerases (21–23). With pol η, the effect of substitution at the O-6 atom is considerably more pronounced than that seen at N-2 (21). With the N^2-alkylG and N^2-aralkylG adducts, the attenuating effect was very limited up to the large N^2-methyl(anthracenyl)G adduct, and the efficiency of insertion of the preferred "wrong" base (A) was also not changed (21). With the O^6-alkylG derivatives (Fig. 11), the addition of a Me group lowered the catalytic efficiency of C incorporation by an order of magnitude, and the efficiency was further lowered by the substitution of a Bz group. However, the efficiency of T incorporation by pol η was increased by the addition of a methyl group at the O-6 position and then decreased by the substitution of larger groups (Fig. 11). With pol ι the efficiency of dCTP incorporation was decreased to a similar extent by a Me or a Bz group and then very strongly decreased for O^6-PobG (Fig. 11). This effect can be compared with the N^2-alkylG results (22) where a very strong decrease in the efficiency of dCTP incorporation was seen with a methyl group (and the effects of Me and Bz groups were similar). With pol κ the efficiency of dCTP incorporation was rather insensitive to the size of substitution at the N-2 atom. Furthermore, the tendency for misincorporation (of dTTP or dGTP) varied little with size (23). However, substitution of the O-6 atom in the present study had a very strong effect on the efficiency of incorporation by pol κ (Fig. 11*D*).

These results and several thermodynamic studies with modified oligonucleotides in the absence of polymerases (58) suggest that certain base pairing schemes may be operative with O^6-alkylG residues, including a 2-hydrogen bond O^6-MeG:T

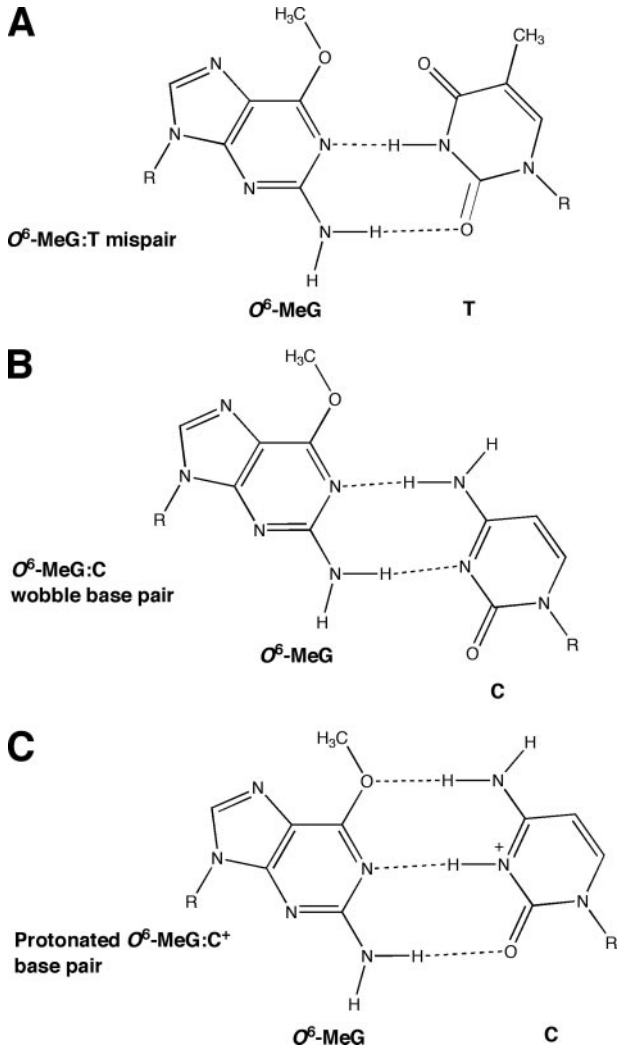

FIGURE 12. **Possible structures of O^6-MeG base pairs.** *A*, O^6-MeG:T mispair. *B*, O^6-MeG:C wobble pair. *C*, protonated O^6-MeG:C$^+$ pair.

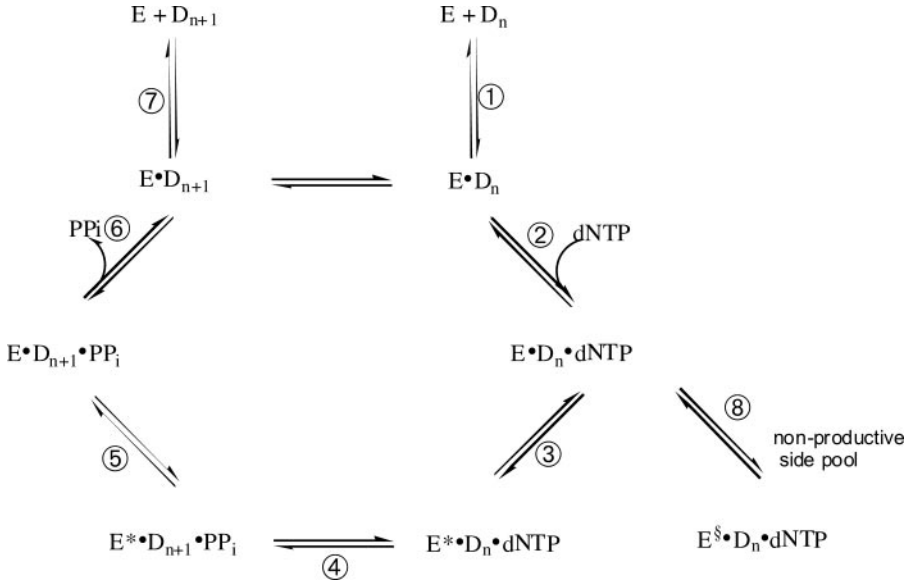

FIGURE 13. **General kinetic mechanism for DNA polymerization.** Individual steps are numbered and discussed in the text. See references (41, 44) and modifications (19, 61). *E* indicates pol; D_n indicates DNA substrate; *E** indicates conformationally altered polymerase; $E^§$ indicates nonproductive conformation of polymerase; D_{n+1} indicates DNA extended by 1 base, and PP_i indicates pyrophosphate.

pair and either a wobble or protonated O^6-MeG:C pair, based on structures of duplex DNA (in the absence of polymerases) determined by x-ray diffraction (58, 59) (Fig. 12). T_m studies show a more favorable free energy for an O^6-MeG:C pair than an O^6-MeG:T pair (58, 60). The thermodynamics of pairing T (dTTP) with O^6-MeG are more favorable than for pairing T with G and are consistent with the increase in k_{cat}/K_m values seen here with all polymerases in going from G to O^6-MeG (Fig. 11). However, the thermodynamics (60) alone cannot explain why the polymerases incorporate dTTP as efficiently or more efficiently than dCTP; this appears to be a kinetic effect imparted by the polymerases.

One issue in understanding the action of polymerases with modified DNA is what steps in the catalytic cycle (Fig. 13) are rate-limiting (46). Analysis of rate-limiting steps in polymerase catalysis requires pre-steady-state kinetic analysis, if possible. A kinetic "burst" for an enzyme reaction provides evidence that the rate-limiting step(s) occur in the first catalytic cycle, followed by a relatively slow step that follows product formation, *e.g.* product release (in a system in which single base insertion is monitored, rather than processive polymerization) (41). In the normal incorporation of dCTP opposite G, pol η, ι, and κ all showed burst kinetics (Figs. 3 and 4), although the patterns are not as sharp as seen with mammalian pol δ (32) and several "model" bacterial DNA polymerases (62, 63). These bursts are lost for incorporation of dCTP opposite O^6-MeG and O^6-BzG (Figs. 3 and 4). In the steady-state kinetic analysis with pol ι, T was preferentially inserted opposite O^6-MeG and O^6-BzG instead of C (Table 2); therefore, dTTP incorporation was analyzed in more detail (Fig. 4). The preference for dTTP insertion opposite O^6-MeG > G was also seen in this mode (Fig. 5*B*). A modest burst character was seen for dTTP insertion opposite O^6-MeG and O^6-BzG (similar to dCTP insertion opposite G) with pol ι.

In all of the cases examined, the absence of sharp kinetic bursts seen with incorporation (of dCTP) opposite the O^6-alkylG adducts implies that steps associated with or occurring prior to product formation (Fig. 13) are rate-limiting. What is not clear is whether the alkylation causes the step involving formation of the phosphodiester bond to become rate-limiting (*step 4* in Fig. 13) or whether a conformational or other step preceding the bond formation step (*e.g.* step 3) is rate-limiting. The absence of sharp bursts in the work with the O^6-MeG and O^6-BzG adducts and Y family DNA polymerases (Figs. 3 and 4) contrasts with the results of studies with the model polymerases HIV-1 RT and pol T7$^-$, where relatively sharp bursts were seen, but the extent of the burst phase was reduced (16, 19). The results of those studies

were interpreted in the context of a kinetic model in which a fraction of the polymerase is in a nonproductive complex(es) in equilibrium with the productive complex (19), which is generally compatible with a recent new model for action of replicative DNA polymerases (64). In comparing the O^6-alkylG burst analyses for the Y family polymerases with the N^2-alkylG adducts, relatively sharp bursts were observed with pol η and κ, even with considerable bulk (21, 23). With pol ι, the burst phase was lost with adducts larger than N^2-ethylG (22).

Our misincorporation results with individual DNA polymerases may be compared with mutagenesis studies in the literature. The literature on O^6-alkylG mutations is dominated by reports of G to A transitions, *i.e.* the result of incorporation of T opposite the adduct (8). However, limited information is available about which DNA polymerases are involved in O^6-alkylG mutagenesis, both in prokaryotic and eukaryotic systems. Also, only very limited mutagenesis studies have been done with O^6-PobG to date (24). In the present study we showed an efficiency of bypass of O^6-PobG in the order pol η > pol δ, ι, and κ, but in any cell the relative roles will depend upon the amounts of these (and any other relevant) DNA polymerases. Although the pol η-catalyzed incorporations opposite O^6-PobG are relatively inefficient (Table 2), they may account for cellular mutations (24); alternatively, other DNA polymerases that we have not included in this study are more involved. All of the DNA polymerases examined here did insert T opposite all of the O^6-alkylG lesions, as expected (Table 2 and Fig. 7). Of these human DNA polymerases, all showed similar efficiencies of insertion of C and T, with two exceptions as follows: (i) pol ι showed a preference of an order of magnitude in inserting T > C, and (ii) with pol η and k (although the efficiencies are lower) the fidelity is actually more favorable (for insertion of C) opposite O^6-PobG than O^6-MeG or O^6-BzG (Table 2). With pol η, analysis of the products of primer extension opposite O^6-BzG produced five separate results as follows: (i) error-free incorporation (~55%; Fig. 7); (ii) insertion of T opposite O^6-alkylG (31%) (Figs. 7 and 9 and Table 4); (iii) a 1-base deletion (2%) (Figs. 7 and 8 and Table 3); (iv) a 2-base deletion (1%) (Fig. 7 and supplemental Fig. S10); and (v) misinsertion of A opposite O^6-BzG (11%) (Figs. 7 and 10 and Table 5). The latter three events were not seen in analysis of the products obtained in copying O^6-MeG and O^6-PobG. The products varied in the extent to which pol η finished elongation even after prolonged incubation (Fig. 7), but these results are not surprising in the context of the results observed with pol η and unmodified oligonucleotides (Fig. 2).

The results of the primer extension opposite the O^6-alkylG residues are of interest in the context of some of the mutation results other than T insertion (G to A transitions) that have been reported in cellular systems. In *E. coli*, O^6-BzG was less miscoding than O^6-MeG (11), consistent with our LC-MS/MS results (Fig. 7). Our own O^6-PobG results (only C and T insertions opposite O^6-PobG) are consistent with mutation studies in *E. coli* but do not explain the more complex mutations (deletions and remote mutations, ~5% total) reported in human embryonic kidney 293 cells (24). However, O^6-BzG produced more complex mutations than O^6-MeG in an H-*ras* sequence in Rat4 cells (9), and the insertions of T and A opposite O^6-BzG were seen in our LC-MS/MS work (Fig. 7). We observed deletions in the LC-MS/MS work with pol η and O^6-BzG but, in contrast to the cellular studies of Bishop *et al.* (9), no nontargeted (base pair) mutations at sites adjoining the adduct. Two outstanding issues are as follows: (i) effects of sequence context

TABLE 4

Observed and theoretical CID fragmentation for pol η T insertion product with O^6-BzG

The assigned sequence was 5′-pAGTGAGGACGCCGA-3′ (Fig. 9). See Ref. 53 for nomenclature of fragments.

Fragment assignment	Observed	Theoretical
5′-pA (a_2-B)	490.1	490.1
5′-pAG (a_3-B)	819.1	819.1
5′-pAGT (a_4-B)	1122.9	1123.1
5′-pAGTG (a_5-B)	1452.0	1452.2
(a_5-B, −2)	725.6	725.6
5′-pAGTGA (a_6-B, −2)	882.1	882.1
5′-pAGTGAG (a_7-B, −2)	1046.5	1046.7
5′-pAGTGAGG (a_8-B, −2)	1211.5	1211.2
5′-pAGTGAGGA (a_9-B, −2)	1367.6	1367.7
5′-pAGTGAGGAC (a_{10}-B, −2)	1512.5	1512.2
(a_{10}-B, −3)	1008.0	1007.8
5′-pAGTGAGGACGCC (a_{13}-B, −3)	1310.4	1310.2
pGTGAGGACGCCGA-3′ (w_{13}, −3)	1367.6	1366.6
pTGAGGACGCCGA-3′ (w_{12}, −3)	1257.1	1256.9
pAGGACGCCGA-3′ (w_{10}, −2)	1569.9	1569.3
(w_{10}, −3)	1046.5	1045.8
pGGACGCCGA-3′ (w_9, −2)	1412.4	1412.7
(w_9, −3)	941.9	941.5
pGACGCCGA-3′ (w_8, −2)	1248.6	1248.2
pACGCCGA-3′ (w_7, −2)	1083.7	1083.7
pCGCCGA-3′ (w_6, −2)	927.2	927.1
pGCCGA-3′ (w_5, −1)	1567.0	1566.3
(w_5, −2)	782.7	782.6
pCCGA-3′ (w_4, −1)	1237.1	1237.2
pCGA-3′ (w_3, −1)	948.2	948.2
pGA-3′ (w_2, −1)	659.1	659.1
pA-3′ (w_1, −1)	329.9	330.1

TABLE 5

Observed and theoretical MS fragmentation for pol η A misinsertion product with O^6-BzG

The assigned sequence was 5′-pAGAGAGGACGCCGA-3′ (Fig. 10). See Ref. 53 for nomenclature of fragments.

Fragment assignment	Observed	Theoretical
5′-pA (a_2-B)	490.1	490.1
5′-pAG (a_3-B)	819.1	819.1
5′-pAGA (a_4-B)	1132.1	1132.2
5′-pAGAG (a_5-B)	1460.9	1461.2
(a_5-B, −2)	730.1	730.1
5′-pAGAGA (a_6-B)	1773.9	1774.2
(a_6-B, −2)	886.6	886.6
5′-pAGAGAG (a_7-B, −2)	1051.1	1051.2
5′-pAGAGAGG (a_8-B, −2)	1216.1	1215.7
5′-pAGAGAGGA (a_9-B, −2)	1372.1	1372.2
5′-pAGAGAGGAC (a_{10}-B, −2)	1516.7	1516.7
(a_{10}-B, −3)	1011.1	1010.8
5′-pAGAGAGGACGC (a_{12}-B, −3)	1216.1	1216.9
5′-pAGAGAGGACGCC (a_{13}-B, −3)	1313.4	1313.2
pGAGAGGACGCCGA-3′ (w_{13}, −3)	1369.9	1369.6
pAGAGGACGCCGA-3′ (w_{12}, −3)	1260.0	1259.9
pGAGGACGCCGA-3′ (w_{11}, −3)	1155.6	1155.5
pAGGACGCCGA-3′ (w_{10}, −3)	1046.1	1045.8
pGGACGCCGA-3′ (w_9, −2)	1413.1	1412.7
(w_9, −3)	941.9	941.5
pGACGCCGA-3′ (w_8, −2)	1248.2	1248.2
pACGCCGA-3′ (w_7, −2)	1083.6	1083.7
pCGCCGA-3′ (w_6, −1)	1855.9	1855.3
(w_6, −2)	927.2	927.1
pGCCGA-3′ (w_5, −1)	1565.8	1566.3
(w_5, −2)	782.7	782.6
pCCGA-3′ (w_4, −1)	1237.1	1237.2
pCGA-3′ (w_3, −1)	948.2	948.2
pGA-3′ (w_2, −1)	659.1	659.1
pA-3′ (w_1, −1)	330.1	330.1

on the misincorporations cannot be excluded, and (ii) other (translesion) DNA polymerases that were not examined here may be responsible for some of the events.

In summary, replication by human Y family polymerases past a set of O^6-alkylG adducts yielded patterns of results that were very distinguishable from those reported previously with N^2-alkylG adducts (21, 23, 50). With all of the individual polymerases, O^6-MeG enhanced the efficiency of dTTP incorporation, as opposed to only decreasing dCTP incorporation (Fig. 11). Of these polymerases, pol η was the most efficient. pol δ was completely blocked by O^6-PobG, but pol η could incorporate opposite this and extend the product. Analysis of the product showed predominantly the expected incorporations of C and T in all cases, but unexpected products were an insertion of A, a -1 deletion, and a -2 deletion in the cases of O^6-BzG adduct, which was not seen with the O^6-MeG and O^6-PobG adducts. The results show the intrinsic role of human pol η with these adducts and the role of adduct size at the guanine O-6 atom. This work also demonstrates the complexity of products that can be generated with a single DNA polymerase (Fig. 7).

Acknowledgments—We thank M. L. Manier for assistance with MS and K. Trisler for help in preparation of the manuscript.

REFERENCES

1. Bauer, K. H. (1928) *Mutationstheorie der Geschwulstenstehung*, Springer-Verlag, Berlin
2. Ramos, K. S., and Moorthy, B. (2005) *Drug Metab. Rev.* **37,** 595–610
3. Mattison, D. R., Shiromizu, K., and Nightingale, M. S. (1983) *Am. J. Ind. Med.* **4,** 191–202
4. Gasiewicz, T. A. (1997) *Neurotoxicology* **18,** 393–413
5. Loveless, A. (1969) *Nature* **223,** 206–207
6. Lawley, P. D. (1984) in *Chemical Carcinogens* (Searle, C. E., ed) 2nd Ed., pp. 325–484, American Chemical Society, Washington, D. C.
7. Singer, B., Chavez, F., Goodman, M. F., Essigmann, J. M., and Dosanjh, M. K. (1989) *Proc. Natl. Acad. Sci. U. S. A.* **86,** 8271–8274
8. Green, C. L., Loechler, E. L., Fowler, K. W., and Essigmann, J. M. (1984) *Proc. Natl. Acad. Sci. U. S. A.* **81,** 13–17
9. Bishop, R. E., Pauly, G. T., and Moschel, R. C. (1996) *Carcinogenesis* **17,** 849–856
10. Pauly, G. T., and Moschel, R. C. (2001) *Chem. Res. Toxicol.* **14,** 894–900
11. Pauly, G. T., Hughes, S. H., and Moschel, R. C. (1995) *Biochemistry* **34,** 8924–8930
12. Pauly, G. T., Hughes, S. H., and Moschel, R. C. (1994) *Biochemistry* **33,** 9169–9177
13. Pegg, A. E., Dolan, M. E., and Moschel, R. C. (1995) *Prog. Nucleic Acids Res. Mol. Biol.* **51,** 167–223
14. Memisoglu, A., and Samson, L. (1997) *Crit. Rev. Biochem. Mol. Biol.* **31,** 405–447
15. Zang, H., Fang, Q., Pegg, A. E., and Guengerich, F. P. (2005) *J. Biol. Chem.* **280,** 30873–30881
16. Woodside, A. M., and Guengerich, F. P. (2002) *Biochemistry* **41,** 1027–1038
17. Voigt, J. M., and Topal, M. D. (1995) *Carcinogenesis* **16,** 1775–1782
18. Reha-Krantz, L. J., Nonay, R. L., Day, R. S., and Wilson, S. H. (1996) *J. Biol. Chem.* **271,** 20088–20095
19. Woodside, A. M., and Guengerich, F. P. (2002) *Biochemistry* **41,** 1039–1050
20. Choi, J.-Y., and Guengerich, F. P. (2004) *J. Biol. Chem.* **279,** 19217–19229
21. Choi, J.-Y., and Guengerich, F. P. (2005) *J. Mol. Biol.* **352,** 72–90
22. Choi, J.-Y., and Guengerich, F. P. (2006) *J. Biol. Chem.* **281,** 12315–12324
23. Choi, J.-Y., Angel, K. C., and Guengerich, F. P. (2006) *J. Biol. Chem.* **281,** 21062–21072
24. Pauly, G. T., Peterson, L. A., and Moschel, R. C. (2002) *Chem. Res. Toxicol.* **15,** 165–169
25. Mijal, R. S., Loktionova, N. A., Vu, C. C., Pegg, A. E., and Peterson, L. A. (2005) *Chem. Res. Toxicol.* **18,** 1619–1625
26. Staretz, M. E., Foiles, P. G., Miglietta, L. M., and Hecht, S. S. (1997) *Cancer Res.* **57,** 259–266
27. Thomson, N. M., Kenney, P. M., and Peterson, L. A. (2003) *Chem. Res. Toxicol.* **16,** 1–6
28. Hecht, S. S. (1998) *Chem. Res. Toxicol.* **11,** 560–603
29. Wang, L., Spratt, T. E., Pegg, A. E., and Peterson, L. A. (1999) *Chem. Res. Toxicol.* **12,** 127–131
30. Borer, P. N. (1975) in *Handbook of Biochemistry and Molecular Biology* (Fasman, G. D., ed) 3rd Ed., pp. 589–590, CRC Press, Cleveland, OH
31. Podust, V. N., Chang, L. S., Ott, R., Dianov, G. L., and Fanning, E. (2002) *J. Biol. Chem.* **277,** 3894–3901
32. Einolf, H. J., and Guengerich, F. P. (2000) *J. Biol. Chem.* **275,** 16316–16322
33. Fien, K., and Stillman, B. (1992) *Mol. Cell. Biol.* **12,** 155–163
34. Goodman, M. F., Creighton, S., Bloom, L. B., and Petruska, J. (1993) *Crit. Rev. Biochem. Mol. Biol.* **28,** 83–126
35. Patel, S. S., Wong, I., and Johnson, K. A. (1991) *Biochemistry* **30,** 511–525
36. Johnson, K. A. (1995) *Methods Enzymol.* **249,** 38–61
37. Zang, H., Goodenough, A. K., Choi, J.-Y., Irminia, A., Loukachevitch, L. V., Kozekov, I. D., Angel, K. C., Rizzo, C. J., Egli, M., and Guengerich, F. P. (2005) *J. Biol. Chem.* **280,** 29750–29764
38. Rozenski, J., and McCloskey, J. A. (2002) *J. Am. Soc. Mass Spectrom.* **13,** 200–203
39. Tan, H. B., Swann, P. F., and Chance, E. M. (1994) *Biochemistry* **33,** 5335–5346
40. Boosalis, M. S., Petruska, J., and Goodman, M. F. (1987) *J. Biol. Chem.* **262,** 14689–14696
41. Johnson, K. A. (1993) *Annu. Rev. Biochem.* **62,** 685–713
42. Johnson, K. A. (2003) in *Kinetic Analysis of Macromolecules, A Practical Approach* (Johnson, K. A., ed) pp. 1–18, Oxford University Press, Oxford, UK
43. Herschlag, D., Piccirilli, J. A., and Cech, T. R. (1991) *Biochemistry* **30,** 4844–4854
44. Eger, B. T., and Benkovic, S. J. (1992) *Biochemistry* **31,** 9227–9236
45. Showalter, A. K., and Tsai, M. D. (2002) *Biochemistry* **41,** 10571–10576
46. Guengerich, F. P. (2006) *Chem. Rev.* **106,** 420–452
47. Ni, J., Pomerantz, S. C., Rozenski, J., Zhang, Y., and McCloskey, J. A. (1996) *Anal. Chem.* **68,** 1989–1999
48. Zang, H., Irminia, A., Choi, J.-Y., Angel, K. C., Loukachevitch, L. V., Egli, M., and Guengerich, F. P. (2006) *J. Biol. Chem.* **281,** 2358–2372
49. Zang, H., Chowdhury, G., Angel, K. C., Harris, T. M., and Guengerich, F. P. (2006) *Chem. Res. Toxicol.* **19,** 859–867
50. Choi, J.-Y., Zang, H., Angel, K. C., Kozekov, I. D., Rizzo, C. J., and Guengerich, F. P. (2006) *Chem. Res. Toxicol.* **19,** 879–886
51. Stover, J. S., Chowdhury, G., Zang, H., Guengerich, F. P., and Rizzo, C. J. (2006) *Chem. Res. Toxicol.* **19,** 1506–1517
52. Choi, J.-Y., Stover, J. A., Angel, K. C., Chowdhury, G., Rizzo, C. J., and Guengerich, F. P. (2006) *J. Biol. Chem.* **281,** 25297–25306
53. Christian, N. P., Reilly, J. P., Mokler, V. R., Wincott, F. E., and Ellington, A. D. (2001) *J. Am. Soc. Mass Spectrom.* **12,** 744–753
54. Lawley, P. D. (1995) *BioEssays* **17,** 561–568
55. Barrows, L. R., and Shank, R. C. (1981) *Toxicol. Appl. Pharmacol.* **60,** 334–345
56. Einolf, H. J., and Guengerich, F. P. (2001) *J. Biol. Chem.* **276,** 3764–3771
57. Connolly, M. L. (1993) *J. Mol. Graphics* **11,** 139–141
58. Swann, P. F. (1990) *Mutat. Res.* **233,** 81–94
59. Leonard, G. A., Thomson, J., Watson, W. P., and Brown, T. (1990) *Proc. Natl. Acad. Sci. U. S. A.* **87,** 9573–9576
60. Gaffney, B. L., and Jones, R. A. (1989) *Biochemistry* **28,** 5881–5889
61. Furge, L. L., and Guengerich, F. P. (1998) *Biochemistry* **37,** 3567–3574
62. Furge, L. L., and Guengerich, F. P. (1997) *Biochemistry* **36,** 6475–6487
63. Fiala, K. A., and Suo, Z. (2004) *Biochemistry* **43,** 2106–2115
64. Tsai, Y. C., and Johnson, K. A. (2006) *Biochemistry* **45,** 9675–9687

Translesion Synthesis across O^6-Alkylguanine DNA Adducts by Recombinant Human DNA Polymerases

Jeong-Yun Choi, Goutam Chowdhury, Hong Zang, Karen C. Angel, Choua C. Vu, Lisa A. Peterson and F. Peter Guengerich

J. Biol. Chem. 2006, 281:38244-38256.
doi: 10.1074/jbc.M608369200 originally published online October 18, 2006